Role of the Crystallite Phase of TiO_2 in Heterogeneous Photocatalysis for Phenol Oxidation in Water

Z. Ding, G. Q. Lu,* and P. F. Greenfield

Department of Chemical Engineering, The University of Queensland, Brisbane Qld 4072 Australia

Received: October 27, 1999; In Final Form: January 31, 2000

A series of TiO_2 samples with different anatase-to-rutile ratios was prepared by calcination, and the roles of the two crystallite phases of titanium(IV) oxide (TiO_2) on the photocatalytic activity in oxidation of phenol in aqueous solution were studied. High dispersion of nanometer-sized anatase in the silica matrix and the possible bonding of Si−O−Ti in SiO_2/TiO_2 interface were found to stabilize the crystallite transformation from anatase to rutile. The temperature for this transformation was 1200 °C for the silica−titania (ST) sample, much higher than 700 °C for Degussa P25, a benchmarking photocatalyst. It is shown that samples with higher anatase-to-rutile ratios have higher activities for phenol degradation. However, the activity did not totally disappear after a complete crystallite transformation for P25 samples, indicating some activity of the rutile phase. Furthermore, the activity for the ST samples after calcination decreased significantly, even though the amount of anatase did not change much. The activity of the same samples with different anatase-to-rutile ratios is more related to the amount of the surface-adsorbed water and hydroxyl groups and surface area. The formation of rutile by calcination would reduce the surface-adsorbed water and hydroxyl groups and surface area, leading to the decrease in activity.

1. Introduction

Heterogeneous photocatalysis, a new wastewater treatment and water purification technique, is a fast growing research area in the past decade.[1,2] The advantages of this technique over the traditional wastewater treatment include complete mineralization and high degradation efficiency in treating nearly any organic compounds at low concentrations.[3] Semiconductors, such as TiO_2, ZnO, ZnS, and SnO_2, have been applied as photocatalysts.[4] Among them, TiO_2 is reported as the most promising one because of its high efficiency, stability, and low cost.[5,6]

There are generally two main crystal phases present in TiO_2 photocatalyst, anatase and rutile. It is commonly believed that anatase is the active phase in photocatalytic reactions. Pure rutile normally shows no activity at all. There are also reports that pure rutile does have some activity, but its performance is dependent on the preparation procedure of the photocatalyst, the nature of the precursor compound,[7] and also on the nature of the organic reactant.[8] The role of rutile in photocatalytic reaction appears important when the photocatalysts have mixed phases, because the comparison of photocatalytic activity is based on the initial reaction rate or reaction rate constant normalized by the amount of active phase. To our knowledge, there is no systematic study on the effect of anatase-to-rutile ratios on the activities of the photocatalysts.

The aim of this study was to investigate the role of crystal phase in photocatalytic oxidation of phenol in water. Two series of TiO_2-based photocatalysts were studied in detail: Degussa P25 and silica−titania (ST). The former is a commercial benchmarking photocatalyst and the latter is a catalyst synthesized in our laboratory. Each photocatalyst was calcined for various lengths of time at various temperatures in order to obtain different ratios of anatase to rutile phases. A systematic surface characterization of these samples was conducted and activities on phenol oxidation were also measured. The surface chemistry characterization on the adsorbed water and hydroxyl groups combined with the activity tests will provide insights into the effects of calcination on the phase transformation and subsequently on the roles of different phases in the reaction.

2.Experimental Section

2.1. Sample Preparation. Two series of samples were prepared starting from P25 and ST. The former was supplied by Degussa and the latter was synthesized by mixing anatase sol and silica (fumed, 14 nm) in a ratio of SiO_2 to TiO_2 of 9/1 by weight. The anatase sol was synthesized following Ichinose's route.[9] First 0.1 M of $TiCl_4$ solution was hydrolyzed with ammonia solution (1:9), and the resulting gel (H_4TiO_4) was washed thoroughly with distilled water. To this titanic acid gel was added 30% of H_2O_2 with a H_2O_2/Ti molar ratio of 4, and the solution was diluted with distilled water to reach a final titania concentration of 0.2 M. The thick solution was stirred overnight and anatase sol was obtained after keeping the solution in an autoclave for 6 h at 100 °C. The anatase sol was thoroughly mixed with silica, dried, and finally calcined at 500 °C for 3 h. The P25 samples were calcined at 700 °C for 3, 6, 36, 72 and 96 h. Samples thus obtained are labeled as P-*t*-*T*, where *t* represents calcination time and *T* represents calcination temperature. The ST samples were calcined at 700, 800, 1000, and 1200 °C for 24 h, and two more samples were calcined at 1200 °C for 72 and 168h. These samples are labeled as ST-*t*-*T*.

2.2. Characterization Techniques. Nitrogen adsorption isotherms of the samples were measured on a gas sorption analyzer (Quantachrome, NOVA 1200). All samples were degassed for 3 h at 300 °C before the analysis. The surface area was calculated by the BET equation and the external surface area was determined by the *t*-plot method.

* To whom all correspondence should be addressed. E-mail: maxlu@cheque.uq.edu.au.

10.1021/jp993819b CCC: $19.00
Published on Web 04/20/2000

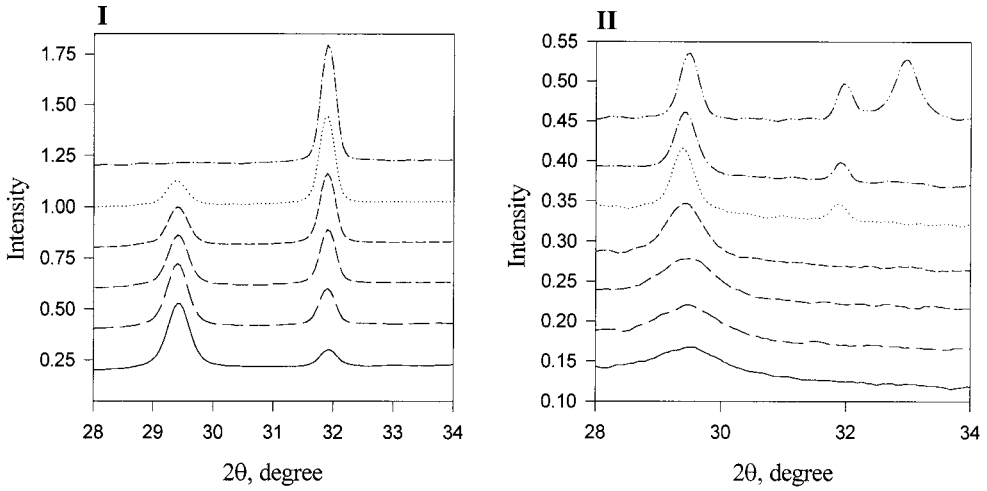

Figure 1. XRD patterns for P25 and ST samples: crystallite transformation. (I) P25 series, from bottom: P25, P-3-700, P-6-700, P-36-700, P-72-700, P-96-700. (II) ST series, from bottom: ST, ST-24-700, ST-24-800, ST-24-1000, ST-24-1200, ST-72-1200, ST-168-1200.

TABLE 1: Concentrations of Anatase and Rutile and Surface Area of Different Photocatalysts

sample	anatase (wt %)	rutile (wt %)	A/R ratio	total surface area (m^2/g)	external surface area (m^2/g)
P25	81	19	4.3	47	41
P-3-700	69	31	2.2	34	30
P-6-700	49	51	0.96	31	27
P-36-700	37	63	0.59	26	23
P-72-700	18	82	0.22	21	19
P-96-700	0	100	0	14	13
ST	7	0	∞	185	154
ST-24-1200	7	0.6	12	3	3
ST-72-1200	7	0.5	14	3	3
ST-168-1200	11	1.5	7.3	3	3

The crystallite phases of the samples were examined by a Philips PW 1840 powder diffractometer (XRD) with cobalt Kα radiation. Standard reference samples with different anatase-to-rutile ratios were prepared from pure anatase and rutile chemicals, purchased from Aldrich Australia, and the calibration curve of the peak intensity against the concentration was used to calculate the amount of anatase and rutile in different samples.[10]

UV−visible diffuse reflectance spectra of samples were recorded on a JASCO 550 UV/vis spectrophotometer with a JASCO ISV-469 integrating sphere accessory, and $BaSO_4$ reference was used.

The surface-adsorbed water and hydroxyl groups on the photocatalyst samples were studied by infrared absorption spectroscopy (Perkin-Elmer FT-IR Spectrometer 2000). The samples were mixed with potassium bromide (KBr) and the concentrations of the samples were kept round 0.25−0.3%. The mixture was pressed under 10 tons/cm^2 to get a 300 mg pellet; 100 scans with a resolution of 2 cm^{-1} were conducted for each pellet. Three conditions were analyzed for each pellet: (I) as prepared, (II) dried for 1 day at 110 °C, and (III) dried for 1 day at 110 °C and then cooled and left in saturated water vapor for 1 h.

The photocatalytic activities of these photocatalysts in degradation of phenol were carried out in a batch reactor.[11] The light source is provided by six UV light tubes (blacklight, 356 nm fluorescent lamps, 8W) for P25 samples and four light tubes for ST samples. The initial phenol concentration was 20 mg/L for P25 and 10 mg/L for ST samples and the concentration of the photocatalyst was 0.1 g/L for P25 and 1 g/L for ST samples.

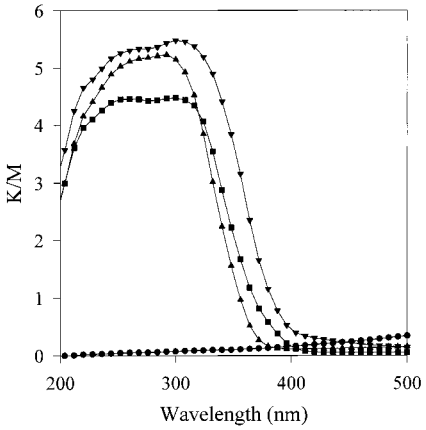

Figure 2. UV-visible spectra of samples: ●, fumed silica; ■, P25; ▲, ST; ▼, TiO_2.

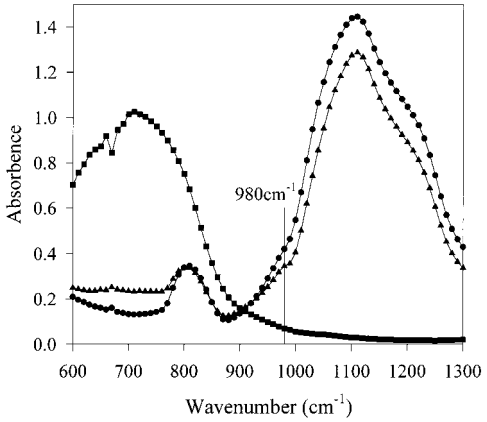

Figure 3. FT-IR spectra of samples: ●, fumed silica; ■, P25; ▲, ST.

3. Results and Discussion

3.1. Effect of Calcination on Crystallite Phase Transformation and Surface Area. The anatase phase of TiO_2 can transform to rutile by calcination at high temperatures, which is shown in Figure 1 for both P25 and ST samples. The peaks at 29.5° 2θ and 32.0° 2θ represent anatase and rutile, respectively.

It can be seen that for P25, this transformation occurs at 700 °C. However, for ST samples calcined at 700 °C, there is no rutile peak detectable. The rutile peak only appears at an elevated temperature of 1200 °C. In addition, the anatase peak areas are

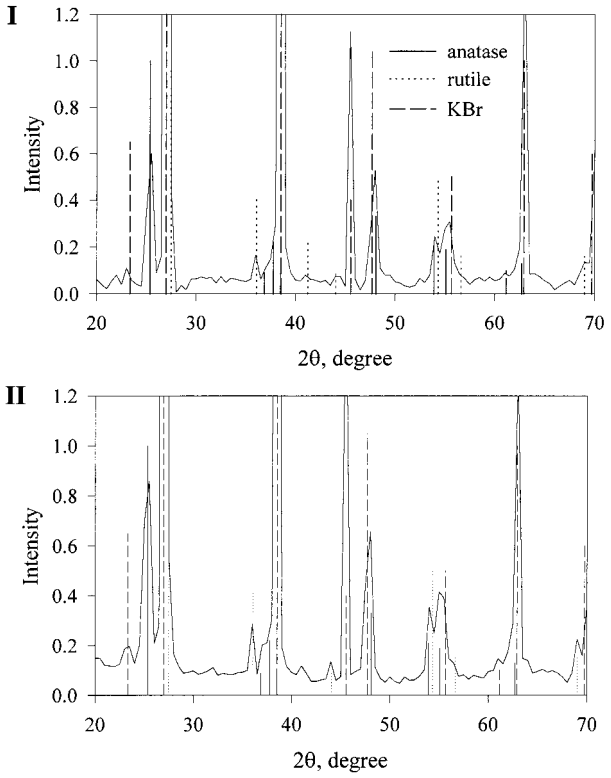

Figure 4. XRD patterns for mixture of KBr and P25 (I) before drying and (II) after drying.

similar with increasing calcination time, while the area of the rutile peak increases significantly with calcination time.

From the broadness of the anatase peaks for P25 and ST, we calculated the anatase crystallite size in both samples,[12] which are 25 and 7 nm, respectively. The concentrations of anatase and rutile and the ratios of anatase to rutile in different samples together with their surface areas are given in Table 1.

Obviously, the ST sample has much finer anatase crystallites than P25. Considering the high SiO_2 to TiO_2 ratio (9/1), one can conclude that these ultrafine anatase crystallites were dispersed well in the silica matrix. The increase of anatase amount upon calcination for ST samples indicates that, in addition to anatase form, there is also little amorphous titania in the starting ST sample. Both of them are separated by the silica matrix, leading to higher energy required for crystallite growth and transformation. More importantly, since anatase is surrounded by silica, there might be Si−O−Ti bonding in the SiO_2/TiO_2 interface, which is reported to be beneficial for stabilization of anatase.[13,14] Figure 2 shows the UV−visible diffuse reflectance spectra of fumed silica, P25, ST, and TiO_2, which was obtained under the same condition as ST but without adding silica.

It is seen that there is a blue shift of the absorption band for ST and P25 compared with the TiO_2 sample, which implies a smaller anatase crystallite size for ST and P25. No obvious peak for isolated Ti species, which have absorption at 210−225 nm, is observed, and the absorption band of ST around 300 nm reflects anatase phase mainly.[15,16] In addition to UV−vis spectroscopic measurement, FT-IR spectra, illustrated in Figure 3 are also obtained to provide information on the interaction between silica and titania.

The spectrum for fumed silica has two bands, one around 1100 cm^{-1} with a shoulder at 1200 cm^{-1} and another around 800 cm^{-1}. These are typical bands for silica, where the former one attributed to asymmetric Si−O stretching and the latter

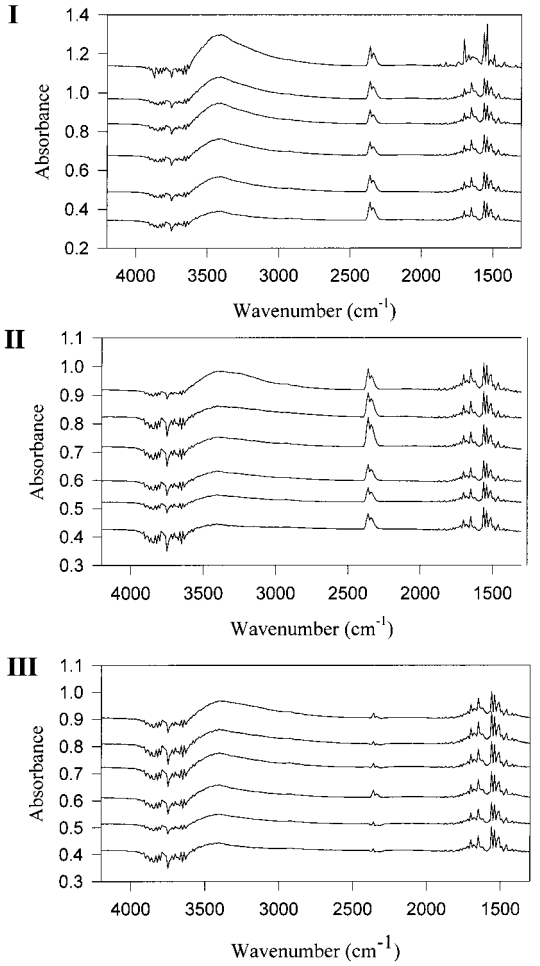

Figure 5. FT-IR spectra of P25 samples. From top, P25, P-3−700, P-6−700, P-36−700, P-72−700, P-96−700: (I) condition I, (II) condition II, and (III) condition III.

attributed to symmetric Si−O stretching. Comparing the spectra for samples P25, fumed silica, and ST, it is seen that ST shows more characteristic bands than silica. Except for those two bands, there is a very small but noticeable shoulder around 980 cm^{-1}. This could be due to the Si−OH stretching vibration[17] or from the bonding of Si−O−Ti,[18] which normally shows a band at around 960 cm^{-1}, indicating the possibility of a Si−O−Ti interaction at the SiO_2/TiO_2 interface. Therefore, ST samples show much higher temperature for the phase transformation. Even at 1200 °C, there is only very little rutile formed.

The specific surface area decreases upon calcination for all samples. For P25 samples, the surface area gradually decreases with calcination time, whereas for ST samples, the surface area is drastically reduced to as low as 3 m^2/g after calcination. This indicates that the fine silica particles agglomerated, resulting in much larger nonporous particles, leading to the decrease in the surface area. In the meantime, anatase crystallite size was also growing, which can be observed through the sharpness of the anatase peak in the XRD patterns.

3.2. Relation between the Crystallite Phase and Surface Water and Hydroxyl Groups. FT-IR analysis is conducted to study the surface chemistry of the photocatalyst samples. First, the possible reaction between KBr and TiO_2 at elevated temperature, 110 °C, was investigated. KBr was mixed with P25 with a ratio of 9:1 by grinding and the XRD pattern was recorded, as shown in Figure 4, for the mixture before and after drying at 110 °C for 1 day.

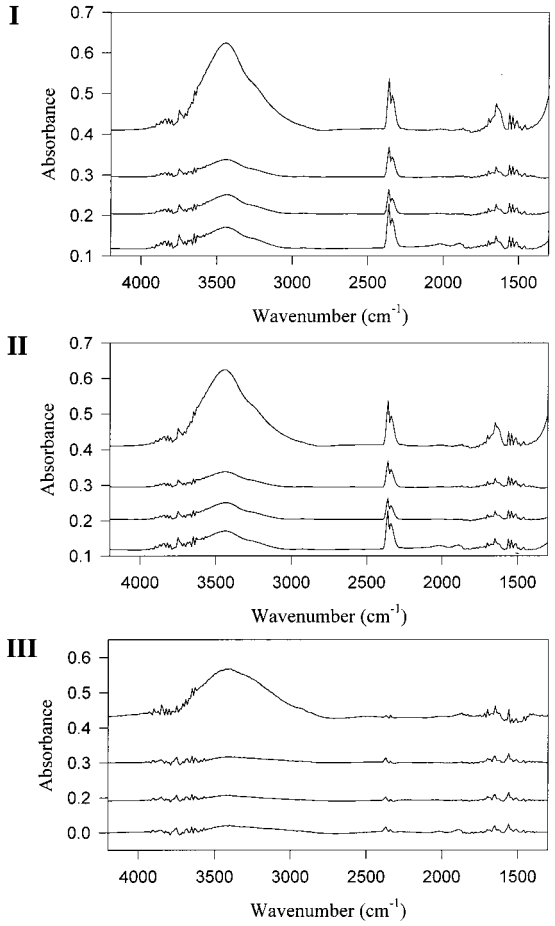

Figure 6. FT-IR spectra of ST samples. From top, ST, ST-24−1200, ST-72−1200: ST-168−1200. (I) condition I, (II) condition II, and (III) condition III.

TABLE 2: Amount of Surface-Adsorbed Water and Hydroxyl Groups in Various Samples under Condition I

sample	absorption intensity (arbitrary unit)	sample	absorption intensity (arbitrary unit)
P25	62.6	ST	94.4
P-3-700	46.4	ST-24-1200	13.2
P-6-700	38.7	ST-72-1200	14.2
P-36-700	34.1	ST-168-1200	16.1
P-72-700	27.7		
P-96-700	9.0		

It is seen that there is not much difference for either peak position or shape for both anatase and rutile phases before and after the mixing and drying. Therefore, we can conclude that no reaction happened between KBr and TiO_2.

Figure 5 shows the FT-IR spectra of P25 samples under three conditions. These spectra show one broad band around 3400 cm^{-1} and one around 1650 cm^{-1}. It has been reported that adsorbed water has bands around 3400 and 1630 cm^{-1},[19−21] while Ti−OH bonding has bands around 3563, 3172, and 1600 cm^{-1}.[22] Moreover, small crystallites could result in the broadness of the peaks.[22] Therefore, it is believed that the two observed

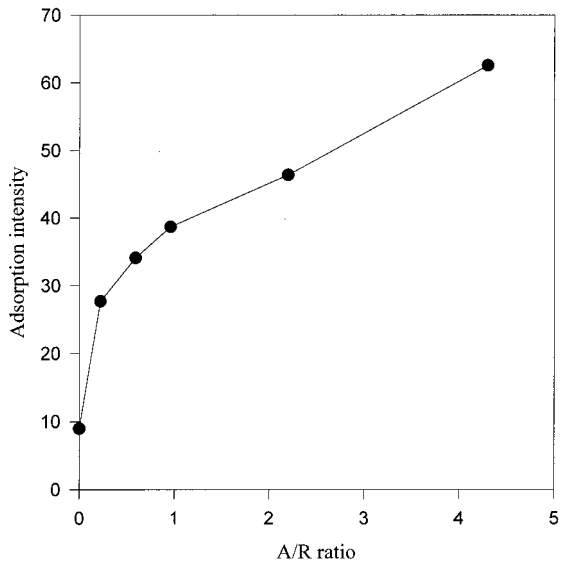

Figure 7. Relation between the amount of the surface adsorbed water and hydroxyl groups and anatase-to-rutile ratios (A/R) for P25 samples.

peaks at 3400 and 1650 cm^{-1} correspond to the surface adsorbed water and hydroxyl groups. The peak around 2400 cm^{-1} is for CO_2 in air, which is not important in this study. FT-IR spectra for ST samples are shown in Figure 6. The positions of the bands are very similar to those of P25 samples. In addition, Si−OH bonding has a band around 3600 cm^{-1}.[19] Therefore, these two bands also represent the surface adsorbed water and hydroxyl groups, and part of them are adsorbed or bonded on silica particles. It has been shown that, when reducing the dilution of the sample in the pellet to 0.25−0.3%, there is a linear relation between the absorption intensity and the amount of adsorbed species in samples.[23] In this work, the peak area at 3400 cm^{-1} under condition I (as prepared) is measured and used to represent the amount of the surface-adsorbed water and hydroxyl groups on both P25 and ST samples, which is shown in Table 2.

As seen from this table, for P25, the increase in the amount of rutile results in the decrease of the surface adsorbed water and hydroxyl groups. This trend is observed for all three conditions, and Figure 7 shows the relation between the absorption intensity measured under condition I and the anatase-to-rutile ratios as a representative. Unlike P25 samples, there is no clear relation between the crystallite phase of titania and the absorption intensity. The reason might be the low surface area of ST samples after calcination, leading to a remarkable decrease in the amount of surface adsorbed water and hydroxyl groups. For photocatalytic reactions, the surface adsorbed water and hydroxyl groups are crucial. They will react with photoexcited holes on the catalyst surface and produce hydroxyl radicals, which is a powerful oxidant in degrading organics in water.[24] In this study, although catalysts are dispersed in phenol aqueous solution, which is quite different from the condition in FT-IR analysis, it is believed that the amount of water and hydroxyl groups on the active sites of the photocatalyst surface is

TABLE 3: Initial Reaction Rates for Phenol Degradation

sample	R_0 (mg L^{-1} h^{-1})	R_s (mg g^{-1} h^{-1})[a]	sample	R_0 (mg L^{-1} h^{-1})	R_s (mg g^{-1} h^{-1})[a]
P25	19.8	198	P-96-700	5.74	57.4
P-3-700	16.8	168	ST	8.88	88.8
P-6-700	15.2	152	ST-24-1200	0.494	4.94
P-36-700	13.9	139	ST-72-1200	1.39	13.9
P-72-700	11.5	115	ST-168-1200	1.46	14.6

[a] R_s, the specific initial reaction rate, is R_0 normalized by the amount of titania.

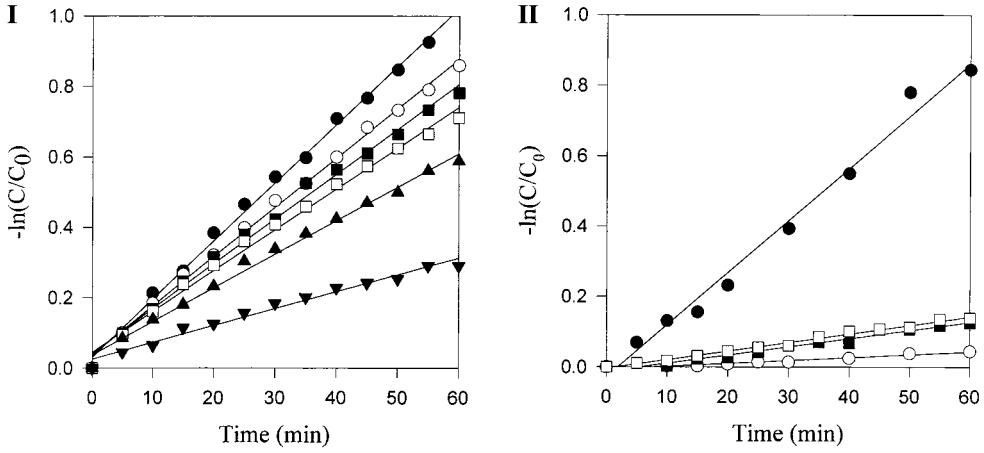

Figure 8. Degradation kinetics of phenol with different sample (I) P25 series: (●) P25, (○) P-3-700, (■) P-6-700, (□) P-36-700, (▲) P-72-700, (▼) P-96-700. (II) ST series: (●) ST, (○) ST-24-1200, (■) ST-72-1200, (□) ST-168-1200.

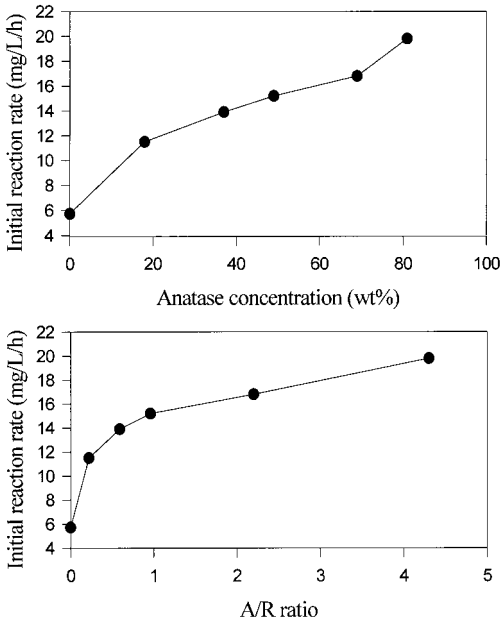

Figure 9. Relation between the initial reaction rate and the amount of anatase and anatase-to-rutile ratios (A/R) for P25 samples.

positively related to the absorption band intensity analyzed with FT-IR. This has been demonstrated by Magrini and co-workers.[25] They showed that modified hydrophobic TiO_2, also supplied by Degussa, has much less activity than P25 in oxidation of trichloroethylene (TCE) in water, though it is thought to have better performance because it can concentrate hydrophobic TCE at the catalyst surface. This shows the importance of adsorbed water and hydroxyl groups on the photocatalyst surface, which is related to the hydrophobicity of the sample. Its effect on the activity of the photocatalyst will be discussed below.

3.3. Photocatalytic Activity. The photocatalytic activities of the P25 and ST series of samples are shown in Figure 8 as the degradation of phenol, $-\ln(C/C_0)$, versus time.

The reaction follows first-order kinetics, and the initial reaction rates are tabulated in Table 3.

By relating initial reaction rate (Table 3) to the concentration of anatase (Table 1), it is seen that for P25 samples, the activity is proportional to the amount of anatase, as shown in Figure 9. In addition, relating the initial reaction rate to the anatase/rutile (A/R) ratios, it is found that before reaching A/R of 1, the activity increases exponentially, while after that point, the activity is linearly related to the A/R ratios. When all anatase is transformed to rutile, the sample still has a certain activity. This indicates that both anatase and rutile contribute to the reaction and anatase is probably more active than rutile. When rutile is abundant in the sample, a little increase in the anatase amount could enhance the activity dramatically.

Unlike P25 samples, ST samples have no such a clear trend. It is difficult to obtain rutile phase in ST samples, and after high temperature calcination, both anatase and rutile amounts are slightly increased. The activities seem to decrease upon

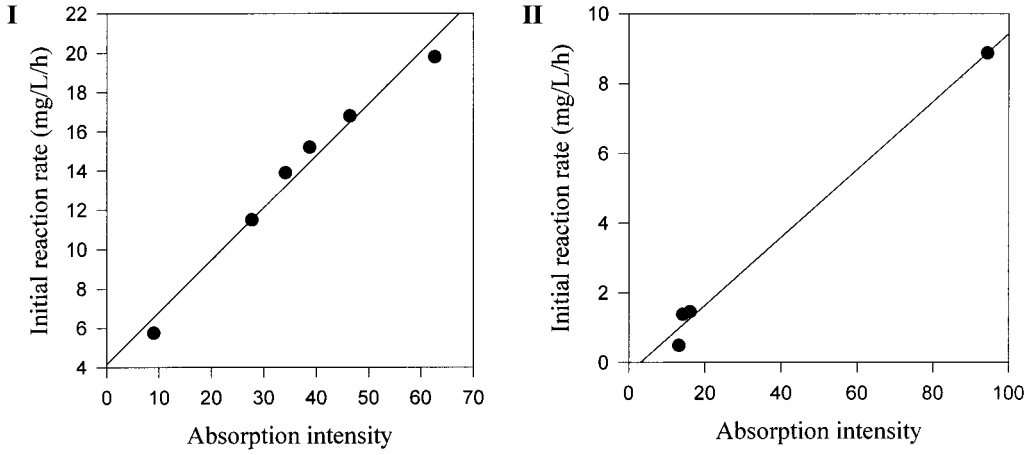

Figure 10. Relation between the initial reaction rate and the amount of the surface adsorbed water and hydroxyl groups for P25 and ST samples: (I) P25 series and (II)ST series.

calcination, possibly attributed to the dramatic reduction in surface area due to sintering.

As mentioned before, the surface-adsorbed water and hydroxyl groups are important in the photocatalytic reaction. The similarity in the relation between initial reaction rate and A/R ratios (Figure 9) with that between surface-adsorbed water and hydroxyl groups and A/R ratios (Figure 7) indicates that the initial reaction rate might be affected by the surface adsorbed water and hydroxyl groups. Figure 10 shows variations of the initial reaction rate with the amount of the surface adsorbed water and hydroxyl groups for both P25 and ST samples.

It can be seen that there is nearly a linear relation between the activity and the amount of the surface adsorbed water and hydroxyl groups, and more importantly, this trend is true for both series of samples. This explains why ST samples have very low activity after calcination. Although these ST samples still have a certain amount of anatase, the amounts of surface adsorbed water and hydroxyl groups were reduced greatly, resulting in the low activities. Titania with anatase, rutile, or mixing crystallite phase is essential to obtain the activity in the photocatalytic reaction. However, the relation between the crystallite phases and activity is very complicated. As shown above, the activity is more related to the surface-adsorbed water and hydroxyl groups. Therefore, it is appropriate to use the initial reaction rate normalized by the amount of titania instead of the amount of anatase for comparison among samples with different compositions. The normalized rates thus obtained are given in Table 3, as R_s. It is noted that the initial reaction rate of the ST sample before calcination is comparable with that of the P25.

4. Conclusion

Samples with different anatase-to-rutile ratios were synthesized, and the relation between the crystallite phases and their activities was studied. From this study, the following conclusions can be drawn: (1) The high dispersion of titania in the silica matrix and possible Si−O−Ti bonding could inhibit the crystallite transformation from anatase to rutile. The transformation temperature is 700 °C for P25 and 1200 °C for ST sample, respectively. In addition to the crystallite transformation obtained by high-temperature calcination, crystallite growing and serious sintering were also observed, leading to the drastic decrease in surface area. (2) The amount of the surface-adsorbed water and hydroxyl groups is related to the crystallite form and surface area. Anatase is more active than rutile in adsorbing water and hydroxyl groups. Surface area also has an important and beneficial effect on the adsorption. (3) Both anatase and rutile are active in the photocatalytic reaction, and the activity of the sample is clearly more related to the surface-adsorbed water and hydroxyl groups.

Acknowledgment. The authors are grateful for the assistance provided Mr. Frank Audsley in XRD measurements. Financial support from the Australian Research Council (ARC) is also gratefully acknowledged.

References and Notes

(1) Ollis, D. F.; Al-Ekabi, H., Eds. *Photocatalytic Purification and Treatment of Water and Air*; Elsevier Science: Lausanne, 1993.
(2) Schiavello, M. *Heterogeneous Photocatalysis*; John Wiley & Sons: Chichester, 1997; Vol. 3.
(3) Serpone, N.; Khairutdinov, R. F. Application of Nanoparticles in the Photocatalytic Degradation of Water Pollutants. In *Semiconductor Nanoclusters*; Kamat, P. V., Meisel, D., Eds.; Elsevier: New York, 1996; Vol. 103; p 417.
(4) Linsebigler, A. L.; Lu, G.; Yates, J. J. T. *Chem. Rev.* **1995**, *95*, 735.
(5) Sclafani, A.; Palmisano, L.; Davi, E. *J. Photochem. Photobiol. A: Chem.* **1991**, *56*, 113.
(6) Legrini, O.; Oliveros, E.; Braun, A. M. *Chem. Rev.* **1993**, *93*, 671.
(7) Sclafani, A.; Palmisano, L.; Schiavello, M. *J. Phys. Chem.* **1990**, *94*, 829.
(8) Tanaka, K.; Hisanaga, T.; Rivera, A. P., *Photocatalytic Purification and Treatment of Water and Air*; Ollis, D. F., Al-Ekabi, H., Eds.; Elservier Science: Lausanne, 1993; p 169.
(9) Ichinose, H.; Terasaki, M.; Katsuki, H. *J. Ceram. Soc. Jpn.* **1996**, *104*, 715.
(10) Spurr, R. A.; Myers, H. *Anal. Chem.* **1957**, *29*, 760.
(11) Ding, Z.; Zhu, H. Y.; Lu, G. Q.; Greenfield, P. F. *J. Colloid Interface Sci.* **1999**, *209*, 193.
(12) Jenkins, R.; Vries, J. L. d. *An Introduction to X-ray Powder Diffractometry*; Philips Gloeilampenfabrieken: Eindhoven, 1970.
(13) Anderson, C.; Bard, A. J. *J. Phys. Chem. B* **1997**, *101*, 2611.
(14) Kumar, S. R.; Suresh, C.; Vasudevan, A. K.; Suja, N. R.; Mukundan, P.; Warrier, K. G. K. *Mater. Lett.* **1999**, *38*, 161.
(15) Anpo, M.; Nakaya, H.; Kodama, S.; Kubokawa, Y.; Domen, K.; Onishi, T. *J. Phys. Chem.* **1986**, *90*, 1633.
(16) Zhang, W.; Froba, M.; Wang, J.; Tanev, P. T.; Wong, J.; Pinnavaia, T. J. *J. Am. Chem. Soc.* **1996**, *118*, 9164.
(17) Blasco, T.; Camblor, M. A.; Corma, A.; Pariente, J. P. *J. Am. Chem. Soc.* **1993**, *115*, 11806.
(18) Gun'ko, V. M.; Zarko, V. I.; Turov, V. V.; Leboda, R.; Chibowski, E.; Holysz, L.; Pakhlov, E. M.; Voronin, E. F.; Dudnik, V. V.; Gornikov, Y. I. *J. Colloid Interface Sci.* **1998**, *198*, 141.
(19) Nakayama, T. *J. Electrochem. Soc.* **1994**, *141*, 237.
(20) Suda, Y.; Morimoto, T. *Langmuir* **1987**, *3*, 786.
(21) Tanaka, K.; White, J. M. *J. Phys. Chem.* **1982**, *86*, 4708.
(22) Sanchez, E.; Lopez, T.; Gomez, R.; Bokhimi; Morales, A.; Novaro, O. *J. Solid State Chem.* **1996**, *122*, 309.
(23) Bertaux, J.; Frohlich, F.; Ildefonse, P. *J. Sedimentary Res.* **1998**, *68*, 440.
(24) Turchi, C. S.; Ollis, D. F. *J. Catal.* **1990**, *122*, 178.
(25) Magrini, K. A.; Goggin, R. M.; Watt, A. S.; Taylor, A. M.; Baker, A. L. *Joint Solar Engineering Conference ASME 1994*, Klett, D. E., Hogan, R. E., Tanaka, T., Eds.; ASME: New York, 1994; p 163.